3′-5′ Exonuclease of Klenow Fragment: Role of Amino Acid Residues within the Single-Stranded DNA Binding Region in Exonucleolysis and Duplex DNA Melting†

Wai-Chung Lam,‡,§ Elizabeth H. Z. Thompson,‡ Olga Potapova,|| Xiaojun Chen Sun,||,⊥ Catherine M. Joyce,*,|| and David P. Millar*,‡

Department of Molecular Biology, MB-19, The Scripps Research Institute, 10550 North Torrey Pines Road, La Jolla, California 92037, and Department of Molecular Biophysics and Biochemistry, Yale University, New Haven, Connecticut 06520

Received November 15, 2001; Revised Manuscript Received January 17, 2002

ABSTRACT: The mechanism of the 3′−5′ exonuclease activity of the Klenow fragment of DNA polymerase I has been investigated with a combination of biochemical and spectroscopic techniques. Site-directed mutagenesis was used to make alanine substitutions of side chains that interact with the DNA substrate on the 5′ side of the scissile phosphodiester bond. Kinetic parameters for 3′−5′ exonuclease cleavage of single- and double-stranded DNA substrates were determined for each mutant protein in order to probe the role of the selected side chains in the exonuclease reaction. The results indicate that side chains that interact with the penultimate nucleotide (Q419, N420, and Y423) are important for anchoring the DNA substrate at the active site or ensuring proper geometry of the scissile phosphate. In contrast, side chains that interact with the third nucleotide from the DNA terminus (K422 and R455) do not participate directly in exonuclease cleavage of single-stranded DNA. Alanine substitutions of Q419, Y423, and R455 have markedly different effects on the cleavage of single- and double-stranded DNA, causing a much greater loss of activity in the case of a duplex substrate. Time-resolved fluorescence anisotropy decay measurements with a dansyl-labeled primer/template indicate that the Q419A, Y423A, and R455A mutations disrupted the ability of the Klenow fragment to melt duplex DNA and bind the frayed terminus at the exonuclease site. In contrast, the N420A mutation stabilized binding of a duplex terminus to the exonuclease site, suggesting that the N420 side chain facilitates the 3′−5′ exonuclease reaction by introducing strain into the bound DNA substrate. Together, these results demonstrate that protein side chains that interact with the second or third nucleotides from the terminus can participate in both the chemical step of the exonuclease reaction, by anchoring the substrate in the active site or by ensuring proper geometry of the scissile phosphate, and in the prechemical steps of double-stranded DNA hydrolysis, by facilitating duplex melting.

The Klenow fragment of DNA polymerase I has two separate enzymatic activities, 5′−3′ polymerase and proofreading 3′−5′ exonuclease, which are located in separate structural domains of the molecule (reviewed in ref *1*). The Klenow fragment is an attractive model system for structure−function studies of a DNA synthesizing enzyme, owing to the availability of high-resolution crystal structures of the enzyme (*2*) and its complexes with DNA substrates (*3*−*8*). The polymerase domain of the Klenow fragment shares sequence homology with other Pol I family (family A) DNA polymerases from prokaryotic, mitochondrial, and eukaryotic sources, and its three-dimensional structure fits the pattern seen throughout the entire polymerase superfamily (*9*, *10*). Sequence motifs that make up the 3′−5′ exonuclease active site are found in proofreading-proficient DNA polymerases from both Pol I and Pol α (family B) groups (*11*, *12*), and the overall three-dimensional structure of the domain is maintained, even when the sequence homology is very limited (*13*). Thus, insights gleaned from studies of the Klenow fragment should be generally applicable to other DNA polymerases.

Cocrystal structures of Klenow fragment−DNA complexes, having the 3′-terminus of either single-stranded or double-stranded DNA substrates bound at the 3′−5′ exonuclease active site, have provided considerable information on the mechanism of the 3′−5′ exonuclease reaction (*3*−*8*). The earliest studies used short single-stranded DNA oligonucleotides complexed with exonuclease-deficient Klenow fragment mutants that were incapable of degrading the substrate. These structural studies, in parallel with site-directed mutagenesis experiments (*3*, *14*, *15*), identified the important components of the 3′−5′ exonuclease active site: the catalytic pair of divalent metal ions, their carboxylate ligands, and amino acid side chains that interact with the unstacked nucleotide bases or sugar−phosphate backbone of the DNA substrate. A subsequent high-resolution crystal structure of wild-type Klenow fragment bound to a heptanucleotide, in which the exonuclease activity was suppressed

† Supported by NIH Grants GM44060 (to D.P.M.) and GM28550 (to C.M.J.).

* Corresponding authors. (C.M.J.) Phone: (203) 432-8992. E-mail: catherine.joyce@yale.edu. (D.P.M.) Phone: (858) 784-9870. E-mail: millar@scripps.edu.

‡ The Scripps Research Institute.

§ Present address: Gen-Probe Inc., San Diego, CA 92121.

|| Yale University.

⊥ Present address: Amgen Inc., Thousand Oaks, CA 91320-1799.

10.1021/bi0120603 CCC: $22.00
Published on Web 02/26/2002

by pH inactivation of the enzyme and by rapid freezing of the cocrystals, confirmed many of the features seen in the earlier structures (*5*). A cocrystal structure of an editing complex of the Klenow fragment with an 11-base pair duplex DNA substrate containing a 3′ overhanging single strand revealed that the 3′-terminus is bound to the exonuclease site in an identical fashion to that seen in the single-stranded DNA complexes, with the duplex portion occupying a cleft between the polymerase and exonuclease domains which is also used in the polymerase mode of binding (*7*, *8*, *16*, *17*). The extent of the single-stranded DNA binding region at the 3′−5′ exonuclease active site implies that three or four base pairs of a fully duplex DNA would need to become melted before binding could occur, consistent with experiments using chemically cross-linked duplex DNAs (*18*). Melting of the terminal three base pairs of a DNA duplex has also been observed in an editing complex cocrystal of bacteriophage RB69 DNA polymerase (Pol α family), even though the relative positions of the polymerase and proofreading domains are very different in the Pol I and Pol α families (*19*).

Although the initial mutational studies of the Klenow fragment and related 3′−5′ exonucleases (summarized in ref *15*) focused on the metal ligands and the amino acid residues that interact with the terminal nucleotide, other side chains within the single-stranded DNA binding region could also participate in the exonuclease reaction. For example, side chains that interact with the penultimate nucleotide could be important for catalysis, either by anchoring the DNA substrate at the exonuclease site or by ensuring proper geometry of the scissile phosphodiester bond. In addition, side chains that are more distant from the point of hydrolysis could facilitate the exonuclease reaction on duplex DNA by stabilizing the binding of the 3−4 bases of single-stranded DNA that result from melting and translocation to the exonuclease site.

In this study, we have introduced mutations into amino acid side chains in the exonuclease domain that have been shown crystallographically to interact with the DNA substrate on the 5′ side of the scissile phosphodiester bond (*4*, *5*). The catalytic activity of the mutant proteins has been measured with both single- and double-stranded DNA substrates in order to assess the role of each side chain in the exonuclease reaction. We have also characterized the mutant proteins using time-resolved fluorescence anisotropy, which is a sensitive technique for measuring the equilibrium distribution of a duplex DNA substrate between the polymerase and exonuclease sites (*20*, *21*). In a previous application of this technique, we demonstrated that mutations in residues that surround the 3′-terminal nucleotide alter the pol-exo partitioning of DNA (*22*). Here, we use this technique to investigate protein side chains that interact upstream of the 3′-terminus and, in some cases, promote binding of a frayed duplex to the 3′−5′ exonuclease site.

MATERIALS AND METHODS

Construction and Purification of Mutant Derivatives of Klenow Fragment. Klenow fragment derivatives having mutations in the 3′−5′ exonuclease domain were constructed, expressed, and purified using procedures described previously (*14*, *15*, *23*). For fluorescence measurements, single mutations were combined with the D424A mutation, which essentially abolishes exonuclease activity (*3*), using standard procedures (*24*). The naming convention used for mutant derivatives is as follows: the residue number is preceded by the one-letter code for the wild-type amino acid and followed by the code for the mutant amino acid.

Table 1: Duplex DNA Sequences[a]

5'-TCGCAGCCGXCAAAATG AGCGTCGGCAGTTTTACATATAGCCGA-5'
5'-TCGCAGCCGXCAAAATG AGCGTCGGCAGTTTTA$_{G}$ATATAGCCGA-5'
5'-TCGCAGCCGXCAAAATG AGCGTCGGCAGTT$_{CCTT}$ATATAGCCGA-5'

[a] X denotes a modified uridine nucleotide with attached dansyl label. Subscripted bases in the sequence indicate mismatches between the primer and template strands.

Oligonucleotide Synthesis and Labeling. Oligonucleotides for fluorescence measurements were synthesized on an automated DNA synthesizer (Pharmacia Gene Assembler Plus) using standard β-cyanoethyl phosphoramidite chemistry and then purified by reversed-phase HPLC using an acetonitrile/triethylammonium acetate eluant system. Dansyl-labeled oligonucleotides were prepared through the use of a protected 5-propylaminodeoxyuridine residue, introduced during automated synthesis. The modified residue was then deprotected and labeled with dansyl chloride, as described previously (*25*).

Sample Preparation. Four oligonucleotide sequences were used for time-resolved fluorescence anisotropy measurements: a 17 nt dansyl-labeled primer strand and three different 27 nt template strands. The template strands were combined with the primer strand to produce three duplexes, containing either 0, 1, or 4 mismatches at the primer 3′-terminus (Table 1). Duplex DNA samples were annealed by mixing 3 μM primer and 3.6 μM template strand in a buffer of 50 mM Tris (pH 7.5) and 3 mM $MgCl_2$. The mixtures were heated to 80 °C for 10 min and allowed to cool slowly to room temperature. Klenow fragment was then added to a final concentration of 4 μM. The protein concentration is at least 100-fold higher than the typical K_d values for these DNA-protein complexes (*26*), ensuring that all DNA is bound.

Time-Resolved Fluorescence Anisotropy. Fluorescence decay curves were measured by the time-correlated single-photon counting method using the instrument described previously (*27*). Samples were excited at 318 nm using the frequency-doubled output from a mode-locked DCM dye laser (Coherent). The resulting emission, collected at right angles to the excitation, was measured at 530 nm with a monochromator (JY H-10) and microchannel plate photomultiplier (Hamamatsu R2809). Horizontally and vertically polarized emission decays were recorded in 512 channels with a time increment of 88 ps/channel. All measurements were performed at a temperature of 20 °C.

The time-dependent fluorescence anisotropy, $r(t)$, was computed from the horizontally and vertically polarized components of the emission ($I_{\parallel}(t)$ and $I_{\perp}(t)$, respectively)

according to eq 1

$$r(t) = \frac{I_{||}(t) - I_{\perp}(t)}{I_{||}(t) + 2I_{\perp}(t)} \quad (1)$$

Anisotropy decays obtained for different combinations of mutant protein and DNA substrate were globally fitted to a two-state model of exposed and buried dansyl probes, corresponding to DNA substrates bound to the polymerase or 3′−5′ exonuclease sites of the Klenow fragment, respectively (*20*, *21*). The fluorescence lifetimes and associated amplitude factors for each probe population were fixed at the values determined previously (*20*). The rotational correlation times and anisotropy amplitudes for each group were linked across all decays and were globally optimized (except for the slow correlation time, which was separately determined for each decay (*26*)). The fraction of buried probes, equivalent to the fraction of DNA primer/templates bound to the 3′−5′ exonuclease site, was locally optimized for each data set. The anisotropy data were assigned appropriate weighting factors according to the values of $I_{||}(t)$ and $I_{\perp}(t)$ at each time point (*20*). The quality of the fits was judged by the global reduced χ^2 value and the local reduced χ^2 values for each data set. A detailed description of the model and the data fitting procedure has been presented elsewhere (*21*).

Calculation of Free Energy Changes. The equilibrium constant describing partitioning of DNA between the polymerase and 3′−5′ exonuclease sites, K_{pe}, is defined in eq 2

$$K_{pe} = \frac{[\text{exo complex}]}{[\text{pol complex}]} = \frac{x_b}{x_e} \quad (2)$$

where x_b and x_e are the fractions of buried and exposed dansyl probes, respectively, recovered from the fluorescence anisotropy analysis ($x_e = 1 - x_b$).

The corresponding Gibbs free energy of partitioning, ΔG°_{pe}, is defined in eq 3

$$\Delta G^\circ_{pe} = -RT \ln K_{pe} \quad (3)$$

where R is the gas constant and T is the absolute temperature.

The change in the free energy of partitioning resulting from a mutation in the exonuclease site, $\Delta\Delta G^\circ_{pe}$, was calculated according to eq 4

$$\Delta\Delta G^\circ_{pe} = -RT \ln (K_{pe}(\text{mutant})/K_{pe}(\text{wild-type})) \quad (4)$$

Exonuclease Assays. 3′−5′ exonuclease activity on single-stranded DNA was assayed by measuring the degradation of 5′-^{32}P-labeled p(dT_{16}) (Amersham Pharmacia Biotech) under steady-state conditions. For most of the enzymes studied, the reaction contained 40 mM Tris·HCl (pH 7.3), 16 mM $MgCl_2$, 0.08 mg/mL bovine serum albumin, 0.4−16 μM DNA 3′-termini, and 0.1 μM enzyme. The Q419A and Y423A mutants required higher substrate concentrations, up to 96 μM DNA, with 1 μM Q419A and 2 or 6 μM Y423A. Samples were removed at appropriate intervals during incubation at 22 °C, quenched by the addition of excess EDTA, and fractionated on a denaturing polyacrylamide-urea gel. The gel was exposed to a phosphoimager to quantitate the radioactivity in the unreacted substrate and in all of the detectable product bands. The number of moles of phosphodiester bonds hydrolyzed at each time point, and hence the reaction rate, was calculated as described previously (*15*). The reaction rate was plotted as a function of DNA concentration and fitted to the Michaelis−Menten equation to determine K_m and k_{cat} (called k_{ss}) for each mutant protein. For wild-type Klenow fragment, the same parameters were also measured under single-turnover conditions. The reaction mixture was the same as described previously except that the concentration of DNA 3′-termini was 16 nM and the enzyme concentration was varied between 0.2 and 10 μM.

The 3′−5′ exonuclease activity on duplex DNA was measured under conditions of enzyme excess so that all the substrate was enzyme-bound and the maximal rate of hydrolysis was attained. The reaction mix was as described previously except that it contained 16 nM labeled p(dT_{16}), annealed to an approximately equimolar concentration (in terms of DNA 3′-termini) of high molecular weight poly(dA). Enzyme concentrations were 1 μM or greater, and the reaction rates were determined as described previously.

RESULTS

Mutant Derivatives of Klenow Fragment. Five mutant derivatives of the Klenow fragment were examined. These contained mutations in amino acid residues located within the 3′−5′ exonuclease domain: Q419, N420, K422, Y423, and R455. The wild-type residues were replaced by alanine to eliminate side-chain interactions that may play a role in DNA binding or exonucleolysis. Structural data for complexes of the Klenow fragment with single-stranded DNA oligonucleotides bound at the exonuclease site (*4*−*6*) show that the side chains of N420 and Y423 interact with the ribose of the penultimate nucleotide, that Q419 and R455 are hydrogen-bonded to the second and third phosphates from the 3′-terminus, respectively, and that K422 interacts with the base of the third nucleotide. Details of these interactions are illustrated in Figure 1.

The kinetic consequences of the aforementioned mutations were investigated using the appropriate single mutants of the Klenow fragment. In addition to the mutations noted previously, all of the Klenow fragment derivatives used for the time-resolved fluorescence anisotropy measurements also contained the 3′−5′ exonuclease-deficient D424A mutation in order to prevent degradation of the DNA substrates. The D424A single mutant served as a reference protein, and the fluorescence anisotropy data for the double mutants (Q419A/D424A, etc.) were compared to this standard.

Enzymatic Activity of the Mutant Proteins. Steady-state kinetic parameters for exonucleolytic cleavage of single-stranded DNA were determined for wild-type Klenow fragment and each mutant derivative, using p$(dT)_{16}$ as a substrate (Table 2). Several lines of evidence, using wild-type Klenow fragment (data not shown), indicate that the k_{ss} values reported in Table 2 correspond to the rate of phosphodiester bond cleavage. First, the pre-steady-state rate did not show burst kinetics when the DNA substrate was 3-fold in excess of enzyme, ruling out the possibility that a step after bond cleavage was rate-limiting. The same conclusion was supported by the observation that the single-turnover rate was equal to the steady-state rate. The possibility that DNA binding itself might be rate-limiting was eliminated by showing that k_{ss} was independent of the

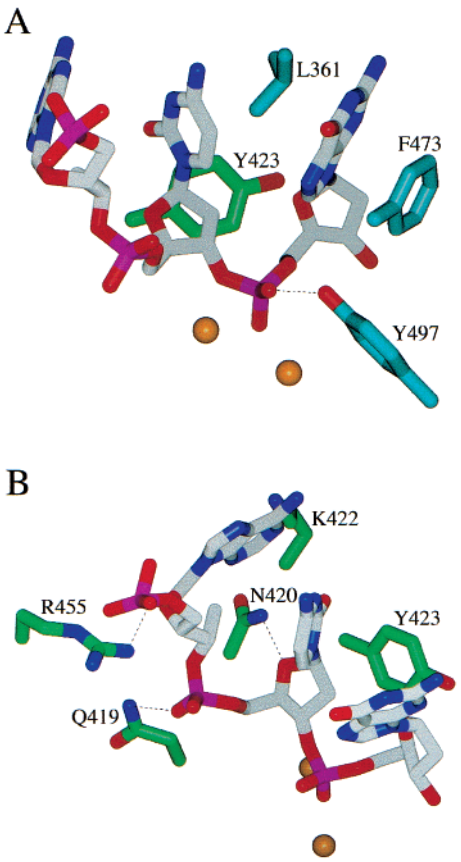

FIGURE 1: Two views of side chains that interact with a single-stranded DNA terminus at the 3′−5′ exonuclease active site of the Klenow fragment: (A) side chains interacting with the terminal nucleotide; (B) side chains that interact with the second and third nucleotides from the 3′-terminus. The coordinates for three nucleotides of DNA bound at the exonuclease site were taken from the Protein Data Bank (pdb file 1KFS) (*5*). Side chains in the present study are shown in green, and those in our previous study (*22*) in dark cyan. The two metal ions interacting with the scissile phosphodiester at the active site are shown as gold spheres. Hydrogen bonds are represented by thin dotted lines. This figure was created using SPOCK (*34*).

concentrations of enzyme and DNA, provided that these concentrations were high enough to ensure saturating conditions. Moreover, if binding were rate-limiting, the association rate constant would correspond to k_{ss}/K_m, and yet, the k_{ss}/K_m values we report are substantially lower than typical association rate constants in other protein−nucleic acid systems (*28*). With phosphodiester hydrolysis as the slow step of the 3′−5′ exonuclease reaction, it follows that the measured K_m gives the binding affinity of the single-stranded substrate and that k_{ss}/K_m is an indication of the efficiency of the reaction.

The largest overall effect on the 3′−5′ exonuclease reaction (measured by k_{ss}/K_m) resulted from the Q419A and Y423A mutations. Both caused a large increase (>200-fold) in K_m; Y423A also gave a 16-fold decrease in k_{ss} relative to wild-type, whereas Q419A had very little effect on the reaction rate. Of the other mutants, N420A also caused a decrease in k_{ss} but hardly any change in K_m, while K422A and R455A had very little effect on exonuclease activity measured with the single-stranded DNA substrate.

The mutant proteins were also assayed for 3′−5′ exonuclease activity on double-stranded DNA (Table 2), using $p(dT)_{16}$ annealed to a poly(dA) template. A standard set of reaction conditions were chosen with wild-type or mutant Klenow fragment at 1 μM, considerably in excess of the concentration of DNA 3′-termini. Because exonuclease digestion by the Klenow fragment of double-stranded substrates is characterized by a very low K_m (*29*), these reaction conditions ensured that all of the DNA was enzyme-bound, a conclusion that was verified by showing that the measured reaction rate was essentially unaffected by a further increase in enzyme concentration. For all of the proteins tested, including the wild-type Klenow fragment, the rate of duplex DNA hydrolysis (k_{ds}) was at least 16-fold slower than k_{ss} (see the ratio in the final column of Table 2). The difference between single- and double-stranded substrates, which has been reported previously (*14*, *30*), has been attributed to at least one additional slow step in the pathway for double-stranded DNA hydrolysis. The effect of the N420A and K422A mutations on duplex DNA hydrolysis paralleled their effect on single-stranded DNA hydrolysis, as shown by k_{ds}/k_{ss} ratios that were similar to the wild-type value. By contrast, Q419A and Y423A showed an even greater reduction in activity on double-stranded DNA than on single-stranded DNA. Interestingly, the R455A mutant protein also showed a significant reduction in exonuclease activity on double-stranded DNA, whereas its activity on single-stranded DNA was similar to that of wild-type Klenow fragment. Thus, Q419, Y423, and R455 appear to be especially important in steps in the reaction pathway that are specific to a double-stranded DNA substrate.

Effect of Mutations on Partitioning of Duplex DNA Between Polymerase and 3′−5′ Exonuclease Sites. Time-resolved fluorescence anisotropy decay experiments were performed to determine whether the mutant proteins are defective in partitioning a duplex DNA substrate from the polymerase site to the 3′−5′ exonuclease site. In these experiments, the fractional occupancies by a DNA substrate of the polymerase and 3′−5′ exonuclease sites are measured using the distinguishable fluorescence anisotropy decay behavior of a dansyl-labeled primer/template duplex bound at each of the two sites (*20*). The dansyl probe is attached to the seventh primer base from the 3′ end (Table 1), a position that gives rise to different local probe environments depending on whether the DNA is bound at the polymerase site or the exonuclease site. When the DNA partitions between both sites, the shape of the resulting anisotropy decay profile is a sensitive function of the relative fractions of DNA bound at the two sites (*20*, *21*).

The 17-nt primer/27-nt template duplex used for these measurements contained a single G·G mismatch at the primer 3′-terminus (Table 1). The presence of the terminal mismatch poises the partitioning equilibrium in a range that is most sensitive to changes resulting from mutations within the protein (*22*). This duplex also serves as a model for the physiological substrate utilized by the Klenow fragment during an editing reaction. In the present experiments, actual cleavage of the DNA substrate was prevented by a D424A mutation, which essentially abolishes the exonuclease activity (*3*).

Representative fluorescence anisotropy decays of dansyl-labeled duplex DNA bound to mutant Klenow fragment derivatives are shown in Figure 2, together with data for the reference protein (containing only the D424A mutation). It is apparent that the anisotropy decay for a given DNA−protein complex is distinct, indicating that substrate partition-

Table 2: 3′−5′ Exonuclease Activity of Klenow Fragment Derivatives

protein[a]	ssDNA k_{ss} (min^{-1})[b]		ssDNA ss K_m (μM)	ssDNA k_{ss}/K_m (M^{-1} min^{-1})	dsDNA k_{ds} (min^{-1})[b]		ratio k_{ds}/k_{ss}
WT	1.1 ± 0.3	[1]	0.64 ± 0.09	1.6×10^6	0.068	[1]	0.06
Q419A	0.63[c]	[0.6]	130[c]	4.8×10^3	0.0029	[0.04]	0.005
N420A	0.080 ± 0.04	[0.07]	1.5 ± 0.7	5.2×10^4	0.0044	[0.06]	0.06
K422A	0.30 ± 0.03	[0.3]	2.7 ± 0.1	1.1×10^5	0.011	[0.2]	0.04
Y423A	(0.07)[d]	[0.06]	(200)[d]	2.2×10^2	0.0001	[0.01]	0.001
R455A	1.3 ± 0.5	[1.2]	2.0 ± 0.2	6.5×10^5	0.0055	[0.08]	0.004
L361A[e]		[0.4]				[0.04]	
F473A[e]		[<0.004]				[0.0003]	
Y497A[e]		[0.03]				[0.06]	
H660A[f]		[0.9]				[0.9]	

[a] WT denotes wild-type Klenow fragment. [b] Rates of ssDNA digestion were the average of three determinations except for Q419A and Y423A. Rates of dsDNA digestion were the average of two determinations. The numbers in square brackets give the rates relative to the corresponding values for wild-type protein. [c] For Q419A, the reaction rate did not reach a plateau value even at 96 μM DNA, the highest concentration tested. The values of k_{ss} and K_m were obtained by fitting the plot of rate versus substrate concentration and are only approximate. [d] For Y423A, the plot of reaction rate versus substrate concentration remained linear up to 96 μM DNA. The slope of this plot gave k_{ss}/K_m; individual values of k_{ss} and K_m were estimated by extrapolation of a double-reciprocal plot and are highly speculative. [e] From refs *14* and *15*; steady-state rates relative to wild-type Klenow fragment, using a slightly different assay protocol. [f] Reaction rate relative to wild-type Klenow fragment, measured under enzyme-excess conditions.

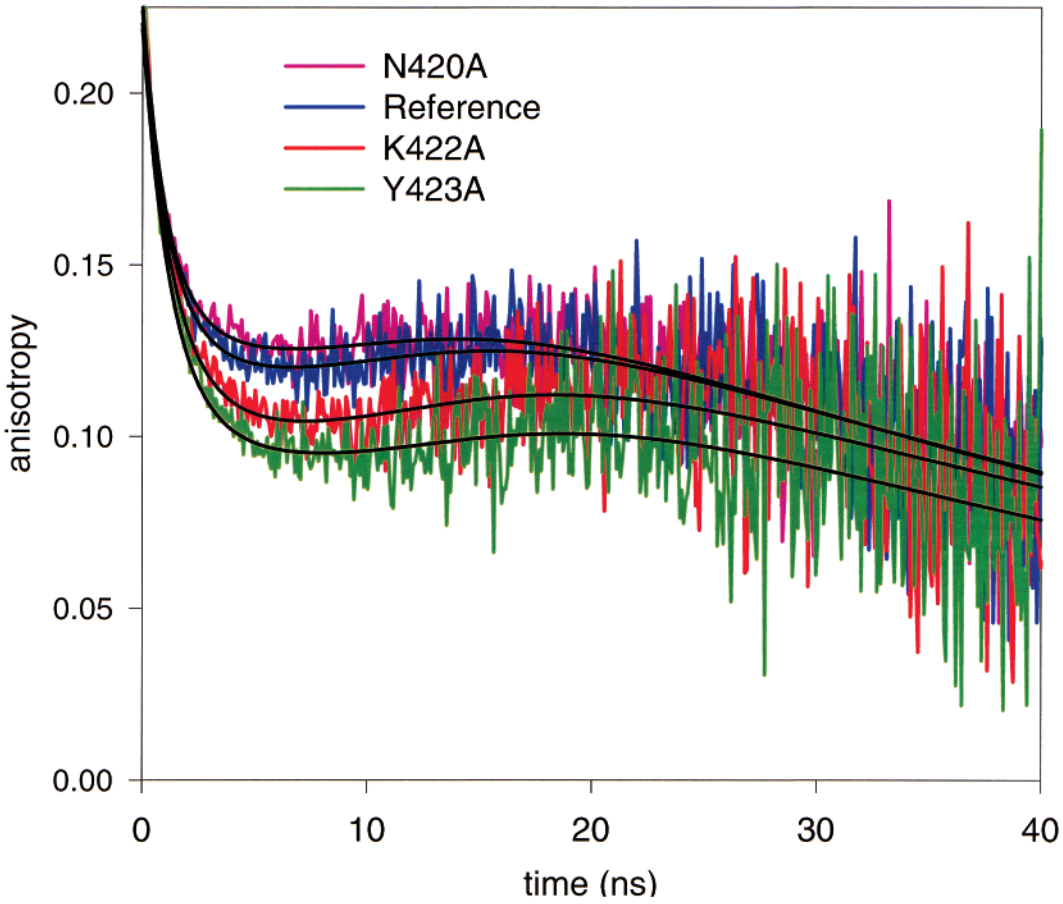

FIGURE 2: Time-resolved fluorescence anisotropy decay profiles of dansyl-labeled primer/template (with terminal G·G mismatch) bound to mutant Klenow fragment derivatives. In addition to the indicated exonuclease domain mutation, each protein also contained the 3′−5′ exonuclease-deficient D424A mutation to prevent DNA degradation. The Klenow fragment derivative used as a reference contained only the D424A modification. The solid lines are from a global best fit to a two-state model of exposed and buried probes, as described in the text. The decays for Q419A and R455A mutant proteins are omitted for clarity.

ing beween polymerase and exonuclease sites is sensitive to mutation of amino acids within the single-stranded DNA binding site. To quantify the differences in partitioning, the set of anisotropy decays were globally analyzed using a two-state model of exposed and buried dansyl probes, corresponding to DNA substrates bound to the polymerase and 3′−5′ exonuclease sites, respectively, as described in Materials and Methods. The global data set also included anisotropy decays of the D424A reference protein bound to primer/templates that were perfectly base paired or contained four terminal mismatches (Table 1). These complexes approximate homogeneous populations of exposed and buried probes, respectively, and were included to constrain the corresponding rotational parameters. An excellent fit was

Table 3: Effect of Mutations on Pol-Exo Partitioning of DNA

mutation	$\Delta\Delta G^\circ_{pe}$ (kJ mol^{-1})[a]	mutation	$\Delta\Delta G^\circ_{pe}$ (kJ mol^{-1})[a]
Q419A	2.3	L361A	3.9[b]
N420A	−0.5	F473A	3.2[b]
K422A	1.5	Y497A	−0.8[b]
Y423A	2.2	H660A	1.8[b]
R455A	1.9		

[a] Change in partitioning free energy resulting from the mutation, as defined in eq 7 in Materials and Methods, and measured with a primer/template duplex containing a single G·G mismatch at the primer terminus (Table 1). Errors are ±0.4 kJ mol^{-1}. [b] Results taken from ref *22*.

obtained, as indicated by a global χ^2 value of 1.08 and by the solid fit lines shown in Figure 2.

The global analysis yielded the equilibrium distribution of the duplex DNA substrate (with G·G mismatch) between the polymerase and exonuclease sites for the reference protein and for each of the mutant Klenow fragment derivatives. These data were used to calculate a $\Delta\Delta G^\circ_{pe}$ value for each mutation, according to eq 7 in Materials and Methods. Under this definition, the $\Delta\Delta G^\circ_{pe}$ value quantifies the change in the partitioning free energy resulting from a mutation to the protein. A positive value of $\Delta\Delta G^\circ_{pe}$ indicates that a mutation favors binding of DNA at the polymerase site, while a negative value indicates that a mutation favors binding at the exonuclease site. The results, shown in Table 3, indicate that most mutations destabilized binding of the DNA substrate at the exonuclease site, consistent with the differences in exonuclease activity on double-stranded versus single-stranded DNA substrates noted previously. The largest effects are observed for the Q419A and Y423A mutations. The R455A mutation also caused a significant defect in partitioning duplex DNA from the polymerase site to the exonuclease site. Interestingly, the N420A mutation had a small stabilizing effect on the binding of the DNA substrate to the exonuclease site.

DISCUSSION

We have created a set of Klenow fragment mutants and characterized their 3′−5′ exonuclease activity in order to probe the role of the corresponding side chains in the mechanism of exonucleolysis. Additionally, we have used time-resolved fluorescence anisotropy to measure the effect of the mutations on the partitioning of a duplex DNA substrate between the polymerase and exonuclease sites and, thus, quantify the energetic importance of protein side chains that contribute to binding DNA at the exonuclease site. We have specifically focused on five side chains (Q419, N420, K422, Y423, and R455) that interact with the DNA substrate on the 5′ side of the scissile phosphodiester bond. With the exception of R455, these residues are part of the conserved Exo II motif (*11*), which also contains one of the carboxylate ligands to the active site metal ions (D424 in the Klenow fragment). Alignment of the Exo II motif in 69 proofreading-proficient DNA polymerases (most from the Pol α family) (*31*) shows that the N420 position is almost invariant (67 out of 69) and that the Y423 position always contains phenylalanine or tyrosine. The K422 position always contains lysine in the subset of bacterial Pol I enzymes that have proofreading capability (20 sequences examined; Joyce, C. M., unpublished observations) but is much less well conserved in the Pol α group. The Q419 residue of the Klenow fragment is even less well conserved; the equivalent residue is glycine in the majority of proofreading-proficient Pol I sequences, but the same position in the Pol α family is usually occupied by an aromatic side chain (H, F, Y, or W). The position equivalent to R455 is also poorly conserved; a basic residue occupies this position in the majority of exonuclease-proficient Pol I enzymes, but a wide variety of different side chains are found in the equivalent position in the Pol α family (*32*). Examination of an editing complex structure of RB69 DNA polymerase (a Pol α family polymerase) suggests that, while the residue aligned with R455 of the Klenow fragment may be different, its function is conserved; thus, S287 of RB69 polymerase, like R455 of the Klenow fragment, interacts with the third phosphate from the 3′-terminus (*19*).

An underlying assumption in the present mutagenesis study is that structural changes in the mutant Klenow fragment derivatives are confined to the positions of the mutated residues. Crystallographic studies have shown this to be true for D424A single-mutant and D355A/E357A double-mutant derivatives of the Klenow fragment (*3*). Moreover, as we have argued previously (*14*), the similar overproduction and chromatographic behavior of wild-type and mutant derivatives suggest that these mutations do not cause substantial perturbations to the overall structure of the enzyme. The fluorescence experiments provide additional supporting evidence in that all the anisotropy decays measured in this study can be readily fitted using a common set of spectroscopic parameters to describe the two environments of the dansyl probe. In view of the strong environmental dependence of the dansyl emission (*27*), this implies that the structural characteristics of the polymerase and exonuclease binding modes are preserved throughout the entire set of mutant protein derivatives.

Cocrystal structures of the Klenow fragment with single-stranded DNA indicate that Q419, N420, and Y423 are in close proximity to the penultimate nucleotide (*4*, *5*). Mutations in these side chains each result in a substantial decrease in exonuclease activity on a single-stranded DNA substrate, indicating that these residues contribute to binding of the single-stranded substrate at the active site or to catalysis of phosphodiester bond cleavage. Q419, which is hydrogen-bonded to a nonbridging oxygen of the penultimate phosphodiester, appears to function primarily in substrate binding, because the Q419A mutation caused a large increase in K_m for cleavage of a single-stranded DNA substrate but little change in the rate constant (Table 2). By contrast, the effect of the N420A mutation is manifested largely in the rate constant for cleavage of single-stranded DNA. The interaction of N420 with O4′ of the sugar of the penultimate nucleotide must, therefore, be important in the transition state of the reaction, perhaps orienting the scissile phosphate in an appropriate geometry for catalysis. As we argue below, this side chain may also introduce strain into the DNA substrate in its ground-state configuration. Y423, whose loss has the most deleterious effect on the exonuclease reaction, appears to play a dual role in the reaction, indicated by the large changes in the values of both K_m and k_{ss} as a result of the Y423A mutation (Table 2). In the crystal structures of the Klenow fragment−oligonucleotide complexes, the side

chain of Tyr423 stacks against the ribose ring of the penultimate nucleotide, and this interaction must be important in both the ground- and transition-states of the enzyme−substrate complex.

The amino acid residues that interact with the DNA substrate upstream from the point of hydrolysis do not appear to participate directly in catalysis. Thus, mutation of R455, whose side chain forms a hydrogen bond with the third phosphodiester from the primer 3′-terminus, has essentially no effect on the exonuclease activity measured on a single-stranded DNA substrate (Table 2). Similarly, removal of the side chain of K422, which interacts with the base of the third nucleotide, has only a modest effect on the catalytic activity. Thus, interactions beyond the penultimate nucleotide do not appear to be particularly important for anchoring single-stranded DNA in the active site or positioning the scissile phosphodiester.

Wild-type Klenow fragment cleaves double-stranded DNA much more slowly than single-stranded DNA, due to the requirement for melting of the duplex terminus and translocation of the DNA from the polymerase site to the 3′−5′ exonuclease site (*14*, *30*). These additional steps are rate-limiting for an exonuclease reaction with a duplex DNA substrate. All five of the mutant proteins in the current study cleaved double-stranded DNA more slowly than the wild-type Klenow fragment (Table 2), indicating that all mutations affect the melting and translocation of a duplex substrate. Two mutations, N420A and K422A, affected the hydrolysis of double-stranded and single-stranded DNAs to a similar degree, as shown by k_{ds}/k_{ss} values that were similar to that obtained with the wild-type protein. By contrast, the Q419A, Y423A, and R455A mutations had much greater effects on the cleavage of a double-stranded DNA substrate than on cleavage of single-stranded DNA, suggesting that these mutations were the most disruptive to the melting or translocation steps in the duplex DNA reaction pathway. Given the location of Q419, Y423, and R455 in proximity to the second and third nucleotides from the 3′ end, it is likely that these residues facilitate duplex melting by stabilizing the binding of the frayed 3′-terminus to the exonuclease site.

The time-resolved fluorescence anisotropy experiments contribute further to understanding the role of the five side chains in this study, by quantifying the energetic consequences of the loss of these side chains. In these experiments, the ability of a mutant protein to melt a duplex DNA substrate and bind the frayed terminus at the exonuclease site is reflected in the equilibrium distribution of the DNA between the polymerase and exonuclease sites. To obtain stable complexes for the time-resolved fluorescence anisotropy measurements, it was necessary to introduce, into all of the proteins examined, the D424A mutation, which essentially abolishes the exonuclease activity but does not measurably affect the partitioning of a primer/template duplex between the polymerase and 3′−5′ exonuclease sites (*22*). Moreover, the mutant proteins were compared with a reference protein which also contained the D424A mutation so that any effects resulting from the D424A mutation would cancel out. Differences in the partitioning behavior of the D424A reference protein and the mutant Klenow fragment derivatives, expressed as $\Delta\Delta G°_{pe}$ values (Table 3), reflect the energetic contributions of individual side chains to binding the frayed DNA terminus at the exonuclease site. These values can be specifically associated with exonuclease site binding, because the mutated side chains do not lie within the duplex binding cleft that is shared between the polymerase and exonuclease modes of binding so that the mutations cannot directly influence the binding of DNA to the polymerase site.

The Q419A, Y423A, and R455A mutations all decreased the fraction of DNA primer/templates bound to the 3′−5′ exonuclease site, corresponding to a significant loss of favorable binding energy (Table 3). These three mutant proteins were more impaired in the hydrolysis of duplex DNA than in hydrolysis of a single-stranded substrate, as shown by the ratio in the final column of Table 2. We therefore infer that interactions with Q419, Y423, and R455 determine not only the strength of binding to the exonuclease site but also the rate at which melting and translocation into the exonuclease site takes place. The R455A mutation is particularly interesting in that it has a negligible effect on the hydrolysis of single-stranded DNA and, yet, appears to play a substantial role in the additional steps that take place with a double-stranded substrate. The interaction between R455 and the third phosphodiester from the 3′-terminus is close to the junction between the frayed single-stranded 3′ end of the DNA duplex in the Klenow fragment editing complex (*7*), and this may account for an important role in melting a duplex substrate. In our previous studies, the L361A mutation also had a greater effect on duplex DNA hydrolysis than on single-stranded DNA hydrolysis, suggesting that L361, which is inserted between the terminal two bases, may also play an important role in melting a double-stranded DNA terminus (*14*, *22*).

The pol-exo partitioning data suggest that N420 functions in a different manner than the other side chains examined here. Rather than destabilizing binding of duplex DNA to the exonuclease site, the N420A mutation actually results in increased occupancy of this site, reflected in a negative value of $\Delta\Delta G°_{pe}$ (Table 3). Thus, the side chain of N420 appears to interfere with binding the DNA terminus at the exonuclease site. A similar effect was previously noted for the Y497A Klenow fragment mutant (*22*). The N420 side chain might orient the DNA substrate in a strained conformation that facilitates catalysis, as suggested previously for Y497. This is consistent with the kinetic parameters for cleavage of single-stranded DNA by the N420A mutant protein (Table 2), which imply that N420 is important in the transition state for cleavage. The Y497 and N420 side chains are located on opposite sides of the scissile phosphodiester, with Y497 hydrogen-bonded to the scissile phosphate and N420 hydrogen-bonded to O4′ of the sugar of the penultimate nucleotide (Figure 3). It is possible that these two side chains act in concert to enforce a strained conformation of the DNA substrate. Given that the N420A and Y497A mutations increase the binding of duplex DNA to the exonuclease site, it is surprising that they decrease the rate of hydrolysis of a duplex DNA substrate. This suggests that N420 and Y497 may contribute positively at an early stage in the binding of a duplex DNA substrate, perhaps during translocation from the polymerase site to the exonuclease site, even though the final bound configuration of the substrate is somewhat destabilized by these two side chains.

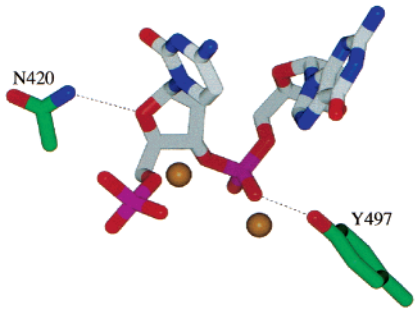

FIGURE 3: Interactions of the N420 and Y497 side chains with a terminal dinucleotide bound to the 3′−5′ exonuclease active site. The two side chains (in green) contribute a net destabilization of the bound substrate and may provide strain that facilitates catalysis. Other details are as described in the legend to Figure 1.

Combining the results of the present study with those from a previous time-resolved fluorescence study (*22*) provides a substantial inventory of interactions between protein side chains and single-stranded DNA at the 3′−5′ exonuclease active site of the Klenow fragment (summarized in Table 3). Aside from the contributions of N420 and Y497, which destabilize binding, there appears to be a correlation between the binding strength and the location of the interaction. Thus, interactions with the 3′-terminal nucleotide (L361 and F473) are the strongest, those with the penultimate nucleotide (Q419 and Y423) are intermediate in strength, and those with the third nucleotide (K422, R455, and H660) are weakest and, in some cases, have little effect on exonuclease reaction rate. The changes in exonuclease cleavage rates, resulting from the mutations described here, are similar in magnitude to those reported previously for other Klenow fragment mutations affecting side chains that interact with the DNA substrate and are, in general, smaller than the effect of mutations that eliminate metal ligands and cause the loss of one or both of the metal ions from the active site (*14*, *15*). Almost all of the side chains we have studied facilitate the melting or translocation of duplex DNA to the 3′−5′ exonuclease active site, though the contribution of side chains that interact with the third nucleotide from the 3′ end is quantitatively smaller. The only exception is H660, whose removal has a negligible effect on the rate of duplex DNA hydrolysis (*22*). Once a frayed single strand is bound at the exonuclease site, side chains surrounding the 3′-terminal two nucleotides participate in a variety of ways: some, like Y423 and Q419, are crucial for binding the substrate or stabilizing the transition state for phosphodiester cleavage, while N420 and Y497 may strain the substrate in a manner that drives hydrolysis of the scissile phosphodiester bond.

Our conclusions concerning the mechanistic roles of the side chains examined in this study complement recent mutational studies of ϕ29 DNA polymerase, a Pol α family polymerase with intrinsic proofreading activity (*31*−*33*). In ϕ29 DNA polymerase, mutations of residues homologous to Q419, N420, and Y423 (H61, N62, and F65, respectively) reduce the 3′−5′ exonuclease activity on single-stranded DNA substrates. Moreover, the mutations have greater effects on duplex DNA hydrolysis than on single-stranded DNA hydrolysis. These results mirror the observations we have made with the corresponding Klenow fragment mutants, although the N62D mutation in ϕ29 polymerase appears to be more disruptive of duplex DNA hydrolysis than we observe for the N420A mutation. Mutations of the Q419 and Y423 homologues in ϕ29 polymerase also weaken the binding of single-stranded DNA to the enzyme, presumably at the 3′−5′ exonuclease site, whereas mutations of the N420A homologue have little effect on binding affinity but appear to result in an abnormal complex. These results agree, qualitatively, with our fluorescence anisotropy data for the corresponding Klenow fragment mutants, which reveal the energetic contributions of these side chains to binding a primer/template duplex at the 3′−5′ exonuclease site. Taken together, these comparisons suggest that residues in the Exo II motif provide similar functions in DNA polymerases from both the Pol I and Pol α families, even though the side chains are not always identical.

REFERENCES

1. Joyce, C. M., and Steitz, T. A. (1994) *Annu. Rev. Biochem. 63*, 777−822.
2. Ollis, D. L., Brick, P., Hamlin, R., Xuong, N. G., and Steitz, T. A. (1985) *Nature 313*, 762−766.
3. Derbyshire, V., Freemont, P. S., Sanderson, M. R., Beese, L., Friedman, J. M., Joyce, C. M., and Steitz, T. A. (1988) *Science 240*, 199−201.
4. Beese, L., and Steitz, T. A. (1991) *EMBO J. 10*, 25−33.
5. Brautigam, C. A., and Steitz, T. A. (1998) *J. Mol. Biol. 277*, 363−377.
6. Freemont, P. S., Friedman, J. M., Beese, L. S., Sanderson, M. R., and Steitz, T. A. (1988) *Proc. Natl. Acad. Sci. U.S.A. 85*, 8924−8928.
7. Beese, L. S., Derbyshire, V., and Steitz, T. A. (1993) *Science 260*, 352−355.
8. Eom, S. H., Wang, J., and Steitz, T. A. (1996) *Nature 382*, 278−281.
9. Steitz, T. A. (1999) *J. Biol. Chem. 274*, 17395−17398.
10. Jager, J., and Pata, J. D. (1999) *Curr. Opin. Struct. Biol. 9*, 21−28.
11. Bernad, A., Blanco, L., Lazaro, J. M., Martin, G., and Salas, M. (1989) *Cell 59*, 219−228.
12. Morrison, A., Bell, J. B., Kunkel, T. A., and Sugino, A. (1991) *Proc. Natl. Acad. Sci. U.S.A. 88*, 9473−9477.
13. Wang, J., Yu. P., Lin, T. C., Konigsberg, W. H., and Steitz, T. A. (1996) *Biochemistry 35*, 8110−8119.
14. Derbyshire, V., Grindley, N. D. F., and Joyce, C. M. (1991) *EMBO J. 10*, 17−24.
15. Derbyshire, V., Pinsonneault, J. K., and Joyce, C. M. (1995) *Methods Enzymol. 262*, 363−385.
16. Doublie, S., Tabor, S., Long, A. M., Richardson, C. C., and Ellenberger, T. (1998) *Nature 391*, 251−258.
17. Li, Y., Korolev, S., and Waksman, G. (1998) *EMBO J. 17*, 7514−7525.
18. Cowart, M., Gibson, K. J., Allen, D. J., and Benkovic, S. J. (1989) *Biochemistry 28*, 1975−1983.
19. Shamoo, Y., and Steitz, T. A. (1999) *Cell 99*, 155−166.
20. Carver, T. E., Hochstrasser, R. A., and Millar, D. P. (1994) *Proc. Natl. Acad. Sci. U.S.A. 91*, 10670−10674.
21. Bailey, M. F., Thompson, E. H. Z., and Millar, D. P. (2001) *Methods* 25, 62−77.
22. Lam, W.-C., Van der Schans, E. J. C., Joyce, C. M., and Millar, D. P. (1998) *Biochemistry 37*, 1513−1522.
23. Joyce, C. M., and Derbyshire, V. (1995) *Methods Enzymol. 262*, 3−13.
24. Sambrook, J., Fritsch, E. F., and Maniatis, T. (1989) *Molecular Cloning: A Laboratory Manual*, Cold Spring Harbor Laboratory, Plainview, NY.
25. Allen, D. J., Darke, P. L., and Benkovic, S. J. (1989) *Biochemistry 29*, 3612−3621.
26. Thompson, E. H. Z., Van der Schans, E. J. C., Joyce, C. M., and Millar, D. P. (2002) *Biochemistry 41*, 713−722.

27. Guest, C. R., Hochstrasser, R. A., Dupuy, C., Allen, D. J. Benkovic, S. J., and Millar, D. P. (1991) *Biochemistry 30*, 8759−8770.
28. Fersht, A. (1985) *Enzyme structure and mechanism*, 2nd ed., W. H. Freeman and Company, New York.
29. Kuchta, R. D., Benkovic, P., and Benkovic, S. J. (1988) *Biochemistry 27*, 6716−6725.
30. Catalano, C. E., Allen, D. J., and Benkovic, S. J. (1990) *Biochemistry 29*, 3612−3621.
31. De Vega, M., Lazaro, J. M., Blanco, L., and Salas, M. (2000) *J. Mol. Biol. 304*, 1−9.
32. De Vega, M., Lazaro, J. M., Salas, M., and Blanco, L. (1998) *J. Mol. Biol. 279*, 807−822
33. De Vega, M., Lazaro, J. M., Salas, M., and Blanco, L. (1996) *EMBO J. 15*, 1182−1192
34. Christopher, J. A. (1998) *SPOCK: The Structural Properties Observation and Calculation Kit (Program Manual)*, The Center for Macromolecular Design, Texas A & M University, College Station, TX.

BI0120603